

Carbon Dioxide Carbonates in the Earth's Mantle: Implications to the Deep Carbon Cycle**

Choong-Shik Yoo,* Amartya Sengupta, and Minseob Kim

Carbon dioxide is an important terrestrial volatile^[1] that is often considered to exist in the deep Earth interior.^[2,3] The presence of carbon dioxide or carbonates in the Earth's mantle strongly affect the stability of partially molten rocks in subducting slabs and magma, and the mantle's physical properties (e.g. density, conductivity, and diffusivity). In various thermal and chemical conditions, carbon dioxide converts into a wide variety of chemical species such as diamond, graphite, carbon monoxide, carbonates, and hydrocarbons.^[4] Thus, the chemical and physical stabilities of carbon dioxide at high pressures and temperatures is critical to understanding the origin and budget of Earth's deep carbon species.^[5]

At pressures above 40 to 60 GPa and temperatures of 300 to 1000 K, carbon dioxide transforms into a range of silicate-like extended solids: four-fold CO₂-V,^[6-8] pseudo-six-fold CO₂-VI,^[9] coesite-CO₂ (*c*-CO₂),^[10] and amorphous *a*-carbonia (*a*-CO₂).^[11] These are fundamentally new solids, consisting of 3D network structures of carbon atoms covalently bonded with oxygen atoms, largely in CO₄ tetrahedra similar to those of silicate minerals.^[12] The large disparity in chemical bonding between the extended network and molecular CO₂, on the other hand, allows these extended solids to exist over a large pressure domain (down to a few GPa) which covers a considerable portion of the Earth's mantle. Carbon dioxide (not extended) dissociates to carbon and oxygen under shock compression at around 4500 K and 34 GPa or at 4600 K and ambient pressure.^[13,14]

Herein, we investigate the transformation of CO₂ phases up to 220 GPa and 2500 K. Above 40 GPa, carbon dioxide transforms into a wide range of covalently bonded extended polymorphs:^[6,9-11] V, VI, *c*, and *a* phases, each with a characteristic Raman-active ν_b (C-O-C) bending vibron at around 700–1000 cm⁻¹ (Figure 1). Upon further compression to 220 GPa, we found that each of these phases became nonmetallic amorphous solids, as evident from the complete

loss of their vibrons and their optical transparency. These amorphous phases remain stable down to 10 GPa, where they slowly transform back to molecular phase I.

Note that pressure-induced amorphization occurs at greatly diverse pressures depending on the phase: for example, CO₂-VI around 95 GPa,^[9] *a*-carbonia around 100 GPa, *c*-CO₂ around 100 GPa, and CO₂-V around 220 GPa (Figure 1). Yet, it is remarkable that amorphization occurs when the ν_b vibron reaches about the same Raman frequency, approximately 1000 cm⁻¹. Based on the pressure dependence of the A_{1g} mode of phase VI and the normalized stishovite vibron, we estimate the ν_b (C-O-C) in a sixfold configuration (CO₆) to be approximately 900 cm⁻¹ at ambient pressure. Therefore, the amorphization may reflect a frustration of strong covalent (sp³ hybridized) C-O bonds to increase either the packing density or the coordination number as pressure increases above 100 GPa.

A similar structural frustration or disorder was observed in CO₂-VI, where carbon atoms are surrounded by an average of six oxygen atoms in a highly distorted octahedron with an average C-O distance of 1.45–1.71 Å,^[9] representing a substantial degree of ionic character in the C-O bonds. Considering the approximately ten percent increase in the Si-O bond length between fourfold quartz (1.61 Å) and six-fold stishovite (1.76–1.81 Å),^[15] we speculate that the C-O bond length must increase to an even larger degree (to 1.65–1.75 Å) to accommodate six oxygen atoms around the smaller carbon atom. With further compression, a separation of this size would eventually lead to structural destruction and the formation of an amorphous solid in which the carbon atoms are highly mixed in coordination but still maintain six or more nearest neighbor atoms. The driving force is then to increase the packing density as apparent from the ν_b mode shifted to approximately 1050 cm⁻¹ (near that of carbonate). Therefore, we attribute the observed amorphization to a similar kind of disorder, driven by the enhanced ionic character of carbon-oxygen bonds and topological densification.

The ionic character of the C-O bonds increases further at high temperatures. Upon laser heating to approximately 1700–1800 K at 85 GPa, all extended phases of CO₂-V, -VI, and *a*-carbonia transform into a new extended ionic solid (depicted as *i*-CO₂) with four characteristic Raman bands at 2000, 1200, 850, and 400 cm⁻¹, as shown in Figure 2 (left and center). Note that *i*-CO₂ is formed only by heating the extended solids above 85 GPa; for example, heating phase III at 55 GPa produces only phase VIII,^[16] whose Raman spectrum consists of two sharp peaks at 800 and 1200 cm⁻¹, without the 2000 cm⁻¹ peak. Upon pressure unloading, *i*-CO₂ remains stable to 10 GPa, below which it slowly converts back into phase I, similar to other extended solids, and confirmed

[*] Prof. Dr. C.-S. Yoo, Dr. A. Sengupta,^[†] Dr. M. Kim
 Department of Chemistry and Institute for Shock Physics
 Washington State University
 Pullman, WA 99164 (USA)
 E-mail: csyoo@wsu.edu
 Homepage: <http://yoo.chem.wsu.edu/>

[†] Present address: Department of Geosciences,
 Princeton University, Princeton, NJ 08544

[**] The present study was supported by NSF (DMR-0854618), DARPA (W911NF-10-1-0081), and DTRA (HDTRA1-09-1-0041). The X-ray work was done at the 16IDB of the HPCAT/APS. We appreciate Dr. Y. Meng for technical support.

Supporting information for this article is available on the WWW under <http://dx.doi.org/10.1002/anie.201104689>.

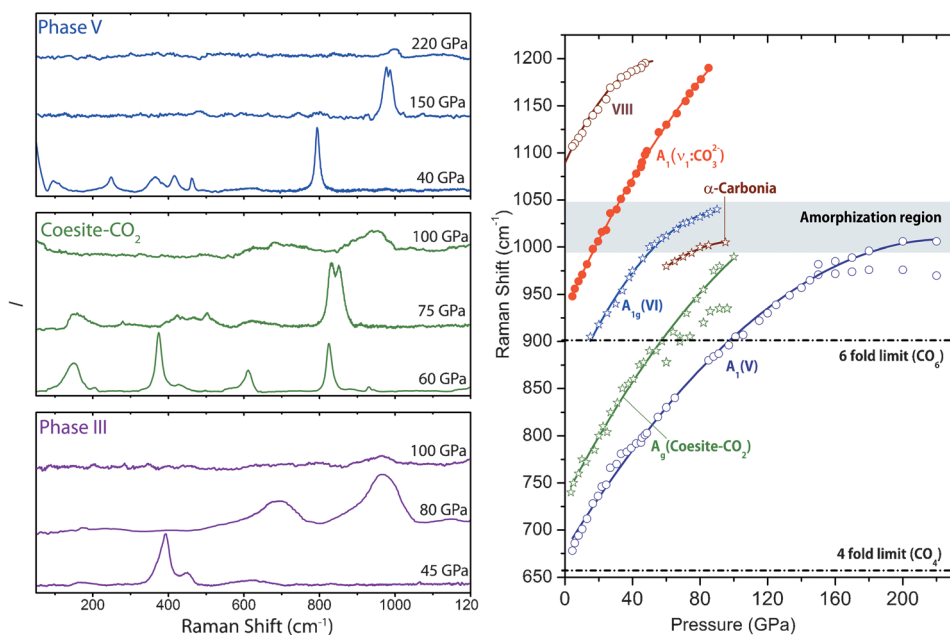


Figure 1. Left: Raman spectra of carbon dioxide phases to 220 GPa, showing the pressure-induced amorphization of top: fourfold CO₂-V via a new high-pressure phase V' above 150 GPa, middle: coesite-CO₂ (c-I) via a high pressure-form (c-II), and bottom: phase III via α -carbonia, at ambient temperature. Right: Pressure dependencies of the major ν_6 vibrons of carbon dioxide phases, illustrating that pressure-induced amorphization occurs well beyond the sixfold vibron limit around 1000–1050 cm⁻¹ (hatched area). The filled red colored circles are the symmetric stretching ν_1 mode of carbonate ions (also in Figure 2).

by the presence of all characteristic Raman peaks. This is in stark contrast to the disordered band of phase VI and a -CO₂ at 2000 cm⁻¹, which disappears at 40 GPa (Figure 2 right).

The Raman spectrum of i -CO₂ is remarkably analogous to those of the previously observed ionic carbonate COCO₃ and nitrate NONO₃ solids.^[17–19] However, there are some differences. For example, both the ν_1 (CO₃) at 980 cm⁻¹ and particularly the ν_s (CO) at 1950 cm⁻¹ appear at substantially lower frequencies than those of ionic solids at 1070 cm⁻¹ and 2220 cm⁻¹, respectively, at approximately 9 GPa (Figure 2 right). Nevertheless, extrapolating the pressure dependence of the ν_1 (NO₃) mode to 85 GPa greatly reduces the difference to within 20–30 cm⁻¹, which easily account for the mass difference. However, the substantially greater difference in the ν_s (CO) mode cannot be explained in terms of pressure dependence or mass difference, but may indicate a local structural difference of carbonyl ions in i -CO₂ from COCO₃.

The Raman spectrum of $i\text{-CO}_2$ is also in contrast to those of theoretically predicted layer structures at this pressure range.^[20–22] In particular, all calculated structures produce several strong extra bands between 700 and 400 cm^{-1} , which are absent in $i\text{-CO}_2$ but present in disordered $a\text{-CO}_2$ and phase VI. Therefore, the absence of such disordered peaks and the above-mentioned large

difference in the $\nu_s(\text{CO})$ suggest a fully extended and more ordered *i*-CO₂ structure.

Our X-ray diffraction data confirms a fully extended nature of ionic carbonate structure. The diffraction patterns of *i*-CO₂ at pressures between 83 GPa and 50 GPa were reasonably well fit to an orthorhombic unit cell: $a = 4.327(5)$, $b = 4.541(5)$, $c = 4.103(4)$ Å, and $\rho = 3.63$ g cm⁻³ at 75 GPa (see Figure 3; for details, see Supporting Information, Figure S1 and Table S1). Based on the Le Bail intensity fittings (Supporting Information, Figure S2), we found that the peak positions are not matched to those of previously reported aragonite structures of CaCO₃ or NONO₃ such as *Pm**cn* or *P2*₁*cn*,^[18,19] but fit reasonably well to the post-aragonite structure *P2*₁*2*₁*2* of CaCO₃,^[23] with a weighted R-factor of 11.6 %. In

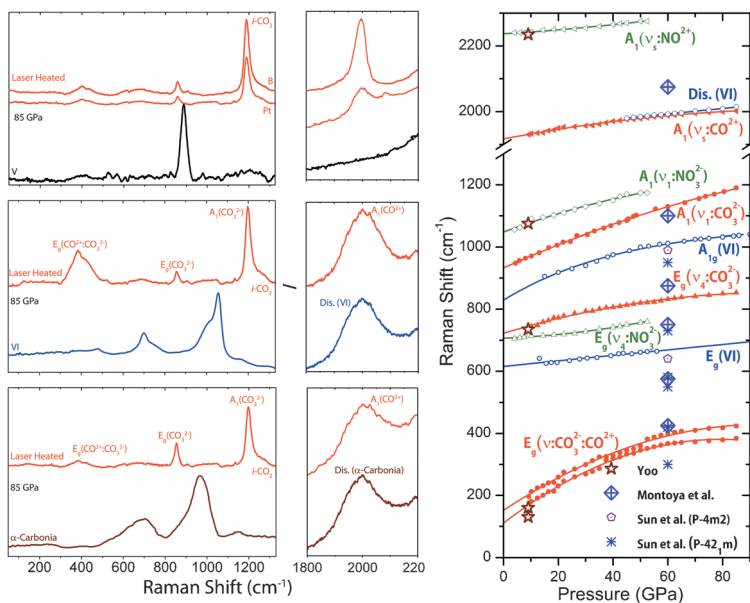


Figure 2. Left and center: Raman spectra of carbon dioxide phases before and after laser heating, showing the transformations of phase V (top), VI (middle), and amorphous *a*-carbonia (bottom) to an extended form of ionic CO₂ carbonates (*i*-CO₂), all at approximately 85 GPa and 1700–1800 K. Indirect Laser heating with Pt and B (top traces in each panel) had no effect on the reaction products, but the broad band at 2000 cm⁻¹ appeared substantially sharper when using a boron heat absorber. Right: Pressure dependence of the Raman spectra of the ionic CO₂ phase (in red solid symbols and lines), plotted together with that of ionic N₂O (green open symbols and lines) for comparison.^[18] Also shown are the Raman spectra of COCO₃ previously synthesized by heating oxygen in carbon at 9 GPa (open stars)^[17] and the calculated Raman spectra of the three-, four-, and mixedfold layered carbonates and *m*-chalcocopyrite structures at 60 GPa (open symbols as labeled at the bottom).^[20–22]

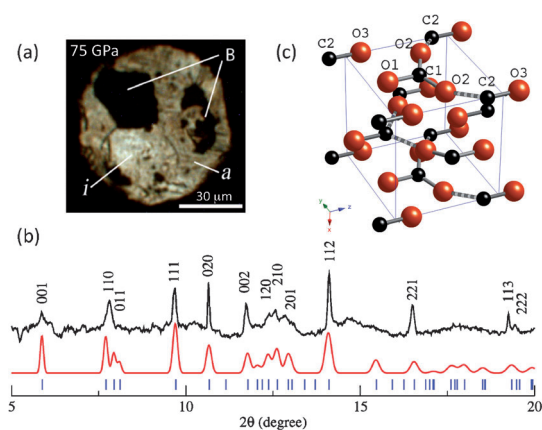


Figure 3. a) A microphotograph of *i*-CO₂ at 75 GPa, produced by indirect laser heating *a*-carbonia by heating boron to approximately 1700 K at 85 GPa. b) The measured (top); background subtracted, and Le Bail fitted (middle) X-ray diffraction of *i*-CO₂ plotted together with the major Bragg reflections (bottom, vertical bars) based on the post-aragonite structure P2₁2₁2. c) The crystal structure of *i*-CO₂ in post-aragonite structure P2₁2₁2. The C black and O red; gray rods are short (1.21 Å) and broken rods long (1.65 Å) C–O bonds, signifying the ionic nature of fully extended structure.

this structure, we used the atomic positions of CO₃ ions exactly same with those of post-aragonite: C1 at 2b(0, 0.5, 0.47), O1 at 2b(0, 0.5, 0.17), and O2 at 4c(0.55, 0.23, 0.40), but those of CO ions replace the Ca site (2a) based on the CO bond length between 0.9 Å and 1.4 Å—a large range of bond lengths that can include various types of CO bonds. Then, the best result (as illustrated in Supporting Information, Figure S3) was obtained at C2(0, 0, 0.85) and O3(0, 0, 0.15), which gives the CO bond lengths of 1.23 Å and C2...O2 interatomic distance of 1.65 Å. Thus, all carbon atoms are quasi-threefold coordinated with oxygen atoms in an extended 2D-layer structure: a half of carbon atoms are bonded to three oxygen atoms at around 1.21(0.1) Å (i.e., CO₃) and the other half at 1.25(0.1) Å with an oxygen atom and 1.65(0.1) Å with the other two in neighboring CO₃ ions, representing ionic bonded (nearly dative) CO to adjacent carbonate ions. On the other hand, such hybridization would certainly soften the ν_s (CO) and ν_1 (CO₃) modes as observed,^[24] and result in a structure remarkably similar to the previously observed “Bridgman Black” polymer (–S–(C=S)–S–)_n at approximately 4.5 GPa and 175 K.^[25] The stability of such 1D polymer (–O–(C=O)–O–)_n containing threefold coordinated carbon atoms has previously been examined to have lower energy by 18 kcal mol^{–1} (per CO₂ unit) than the fourfold extended solid at ambient pressure.^[26]

The present results indicate enhanced stability of *i*-CO₂ carbonates in the pressure-temperature conditions of the Earth’s deep mantle. Based on present and previous data, we construct the phase/chemical transformation diagram (Figure 4), to signify: 1) the formation of *i*-CO₂ above 85 GPa and 1700 K (open circle with vertical arrow), 2) the pressure-induced amorphization at ambient temperature and 100–220 GPa (open circles with horizontal arrows), 3) the formation of carbonyl carbonate (COCO₃) previously observed upon heating carbon in O₂ at 9 GPa and

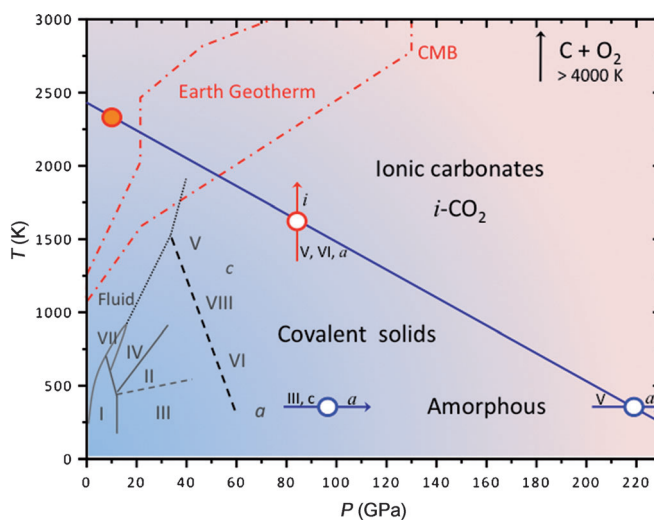


Figure 4. Chemical and phase stability field diagram of carbon dioxide at high pressures and temperatures, signifying the increase in ionic character in carbon dioxide at high pressures and temperatures. The blue and red arrows indicate the amorphization of phases III, c, and V around 100 and 220 GPa and the ionization of phases V, VI and a at 85 GPa and approximately 1700 K, respectively. The dashed lines signify the kinetic lines. The arrow at the right hand corner assumes the decomposition of CO₂ above 4000 K at around 200 GPa.^[13,14] The upper and lower limits of the earth geotherms (red dashed line) and the pressure of the core–mantle boundary are also shown.^[27] See text for details.

2300 K (closed circle), and 4) decomposition of carbon dioxide to carbon and oxygen at high pressures and temperatures based on the extrapolation of shock-induced decomposition of CO₂ at 4600 K and ambient pressure, and 4500 K at 34 GPa.^[13,14] Other phase boundaries are also reproduced, as well as the upper and lower limits of the Earth’s geotherms (red dashed line).^[27] Clearly, the stability of *i*-CO₂ over a large pressure-temperature region relevant to the Earth’s mantle and core, strongly advocates for the possibility of the incorporation of volatile carbon dioxide deep in the Earth’s interior (Supporting Information Figure S4).

In conclusion, we have discovered extended ionic CO₂ solids over broad pressure–temperature conditions, relevant to the Earth’s mantle. The presence of ionic extended solids and CO₂ decomposition products provides an alternative chemical mechanism for the delivery of light elemental impurities, such as oxygen or carbon, from greenhouse gas CO₂ to carbonates in the ocean bottom and the Earth’s crust by mineralization. They are then transformed to extended CO₂ in descending slabs into the deep mantle by carbonate mineral dissociation. Eventually, extended CO₂ in Earth’s core–mantle boundary decomposes to oxygen and carbon, thereby, forming deep carbon species (such as Fe₃C)^[28] in the Earth’s outer core. While extended CO₂ is stable to very low pressures, it converts back into gaseous CO₂ at ambient pressure, which plumes out in volcanic activities but is singled out from many observed surface minerals. Finally, the increased ionic character of the C–O bonds at around 100 GPa suggests that the assumption of strong covalent C–O bonds and high stability of CO₄ tetrahedra to nearly

1000 GPa,^[21] particularly at elevated temperatures, must be revisited, and indicates future studies are required on the long- and short-range structures of disordered extended carbon dioxide at megabar pressures.

Received: July 6, 2011

Published online: September 26, 2011

Keywords: amorphization · carbon dioxide · deep carbon cycle · extended CO₂ carbonates · pressure-induced ionization

- [1] A. E. Saal, E. H. Hauri, C. H. Langmuir, M. R. Perfit, *Nature* **2002**, 419, 451.
- [2] M. Schrauder, O. Navon, *Nature* **1993**, 365, 42.
- [3] M. Isshiki, T. Irifune, T. Hirose, S. Ono, Y. Ohishi, T. Watanuki, E. Nishibori, M. Takata, M. Sakata, *Nature* **2004**, 427, 60.
- [4] A. Y. Nakajima, E. Takahashi, T. Suzuki, K.-I. Funakoshi, *Phys. Earth Planet. Inter. Int.* **2009**, 174, 202.
- [5] R. Dasgupta, M. M. Hirschmann, *Earth Planet. Sci. Lett.* **2010**, 298, 1.
- [6] V. Iota, C. S. Yoo, H. Cynn, *Science* **1999**, 283, 1510.
- [7] C. S. Yoo, H. Cynn, F. Gygi, G. Galli, V. Iota, M. F. Nicol, S. Carlson, D. Hausermann, C. Mailhot, *Phys. Rev. Lett.* **1999**, 83, 5527.
- [8] S. Serra, C. Corazon, G. L. Chiarotti, S. Scandolo, E. Tossatti, *Science* **1999**, 284, 788.
- [9] V. Iota, C. S. Yoo, J. H. Klepeis, Z. Jenei, W. Evans, H. Cynn, *Nat. Mater.* **2007**, 6, 34.
- [10] A. Sengupta, C. S. Yoo, *Phys. Rev. B* **2010**, 82, 012105.
- [11] M. Santoro, F. A. Gorelli, R. Bini, G. Ruocco, S. Scandolo, W. A. Crichton, *Nature* **2006**, 441, 857.
- [12] R. J. Hemley, *High Pressure Research in Mineral Research* (Eds.: M. H. Manghnani, Y. Syono), Terra Sci., AGU, Washington, DC, **1987**, p. 347.
- [13] W. J. Nellis, A. C. Mitchell, F. H. Ree, M. Ross, N. C. Holmes, R. J. Trainor, D. J. Erskine, *J. Chem. Phys.* **1991**, 95, 5268.
- [14] M. A. Oehlschlaeger, D. F. Davidson, J. B. Jeffries, R. K. Hanson, *Z. Phys. Chem.* **2005**, 219, 13.
- [15] D. Andrault, G. Fiquet, F. Guyot, M. Hanfland, *Science* **1998**, 282, 720.
- [16] A. Sengupta, C. S. Yoo, *Phys. Rev. B* **2009**, 80, 014118.
- [17] C. S. Yoo, *Science and Technology of High Pressure* (Eds.: M. H. Manghnani, W. J. Nellis, M. Nicol), Univ. Press, Hyderabad, India, **2000**, p. 86.
- [18] C. S. Yoo, V. Iota, H. Cynn, M. Nicol, J. H. Park, T. Le Bihan, M. Mezouar, *J. Phys. Chem. B* **2003**, 107, 5922.
- [19] M. Somayazulu, A. Madduri, A. F. Goncharov, O. Tschauner, P. F. McMillan, H.-K. Mao, R. J. Hemley, *Phys. Rev. Lett.* **2001**, 87, 135504.
- [20] J. A. Montoya, R. Rousseau, M. Santoro, F. Gorelli, S. Scandolo, *Phys. Rev. Lett.* **2008**, 100, 163002.
- [21] M.-S. Lee, J. A. Montoya, S. Scandolo, *Phys. Rev. B* **2009**, 79, 144102.
- [22] J. Sun, D. D. Klug, R. Mortonak, J. A. Montoya, M. S. Lee, S. Scandolo, E. Tosatti, *Proc. Natl. Acad. Sci. USA* **2009**, 106, 6077.
- [23] S. Ono, T. Kikegawa, Y. Ohishi, J. Tsuchiya, *Am. Mineral.* **2005**, 90, 667.
- [24] T. Shimanouchi, *J. Phys. Chem. Ref. Data* **1977**, 6, 993.
- [25] P. W. Bridgman, *Proc. Am. Acad. Arts Sci.* **1942**, 74, 399.
- [26] G. Frapper, J.-Y. Saillard, *J. Am. Chem. Soc.* **2000**, 122, 5367.
- [27] A. M. Dziewonski, D. L. Anderson, *Phys. Earth Planet. Inter.* **1981**, 25, 297.
- [28] J. Li, C. B. Agee, *Nature* **1996**, 381, 686.